END

FILMED

DTIC

MICROCOPY RESOLUTION TEST CHART
NATIONAL BUREAU OF STANDARDS-1963-A

A Gerdien Condenser System for Measuring
Stratospheric Charged Particle Densities

C. SHERMAN
A.D. BAILEY
J. BORGHETTI

AD-A143 317

3 February 1984

DTIC
ELECTE
JUL 2 0 1984
B

DTIC FILE COPY

84 07 10 028

"This technical report has been reviewed and is approved for publication"

FOR THE COMMANDER

(Signature)
ROCCO S. NARCISI
Branch Chief

(Signature)
ROBERT A. SKRIVANEK
Acting Division Director

Qualified requestors may obtain additional copies from the Defense Technical Information Center.

If your address has changed, or if you wish to be removed from the mailing list, or if the addressee is no longer employed by your organization, please notify AFGL/DAA, Hanscom AFB, MA 01731. This will assist us in maintaining a current mailing list.

Do not return copies of this report unless contractual obligations or notices on a specific document requires that it be returned.

REPORT DOCUMENTATION PAGE

1a. REPORT SECURITY CLASSIFICATION	1b. RESTRICTIVE MARKINGS
Unclassified	
2a. SECURITY CLASSIFICATION AUTHORITY	3. DISTRIBUTION/AVAILABILITY OF REPORT
	Approved for public release;
2b. DECLASSIFICATION/DOWNGRADING SCHEDULE	distribution unlimited.

4. PERFORMING ORGANIZATION REPORT NUMBER(S)	5. MONITORING ORGANIZATION REPORT NUMBER(S)
AFGL-TR-84-0046 IP, No. 322	
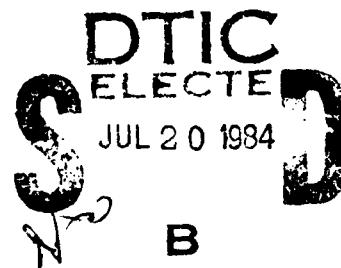
6a. NAME OF PERFORMING ORGANIZATION	6b. OFFICE SYMBOL (If applicable)	7a. NAME OF MONITORING ORGANIZATION
Air Force Geophysics Laboratory	LID	

6c. ADDRESS (City, State and ZIP Code)	7b. ADDRESS (City, State and ZIP Code)
Hanscom AFB Massachusetts 01731	

8a. NAME OF FUNDING/SPONSORING ORGANIZATION	8b. OFFICE SYMBOL (If applicable)	9. PROCUREMENT INSTRUMENT IDENTIFICATION NUMBER

8c. ADDRESS (City, State and ZIP Code)	10. SOURCE OF FUNDING NOS.			
	PROGRAM ELEMENT NO.	PROJECT NO.	TASK NO.	WORK UNIT NO.
	62101F	6687	668703	66870302

11. TITLE (Include Security Classification) A Gerdien Condenser System for Measuring Stratospheric Charged Particle Densities

12. PERSONAL AUTHOR(S) C. Sherman, A.D. Bailey, J. Borghetti

13a. TYPE OF REPORT	13b. TIME COVERED	14. DATE OF REPORT (Yr., Mo., Day)	15. PAGE COUNT
Scientific - Interim	FROM Oct 79 TO Oct 83	1984 February 3	29

16. SUPPLEMENTARY NOTATION

17. COSATI CODES			18. SUBJECT TERMS (Continue on reverse if necessary and identify by block number)
FIELD	GROUP	SUB. GR.	Stratosphere
04	01		Charged particle densities

19. ABSTRACT (Continue on reverse if necessary and identify by block number)

A Gerdien condenser system for measuring stratospheric charged particles densities is described. The system makes use of commercially available blowers to obtain the bulk gas flow through the condenser and a time of charge method for measuring collected currents. System modifications made over several balloon flights are described and the results of one flight are presented in some detail.

20. DISTRIBUTION/AVAILABILITY OF ABSTRACT	21. ABSTRACT SECURITY CLASSIFICATION
UNCLASSIFIED/UNLIMITED ☒ SAME AS RPT. ☐ DTIC USERS ☐	Unclassified

22a. NAME OF RESPONSIBLE INDIVIDUAL	22b. TELEPHONE NUMBER (Include Area Code)	22c. OFFICE SYMBOL
Christopher Sherman	617-861-2525	AFGL/LID

DD FORM 1473, 83 APR   EDITION OF 1 JAN 73 IS OBSOLETE.   Unclassified

Preface

Thanks to Pat Bench for aid in reducing the data and preparation of the graphs.

DTIC
S ELECTED
JUL 2 0 1984
B

3

Contents

Illustrations

5

A Gerdien Condenser System for Measuring
Stratospheric Charged Particle Densities

1. INTRODUCTION

The Gerdien condenser, designed to measure ambient charged particle number densities, was included as a support instrument on our Balloon-Borne Ion Mass Spectrometer payload. It was fabricated as a low budget item using in-house personnel and readily available materials.

A major concern in such measurements has been in obtaining an adequate, known volumetric air flow at the attenuated stratospheric densities. Other workers[1] have accomplished this by use of specially designed positive displacement lobe type pumps not commercially manufactured. We attempted to avoid the fabrication of our own pumps by using a readily available commercially manufactured blower fan. Although attaining required flows and dependability with such fans is not a completely straightforward task, the results so far have been encouraging. The indications are that with further effort the problems encountered can be overcome and the system operated successfully to make stratospheric ion density measurements.

---

1. Rosen, J. M., and Hofmann, P. J. (1981) Balloon borne measurements of the small ion concentration, J. Geophys. Res. 86:7399.

2. INSTRUMENTATION

2.1 Overall System Description

In principal, obtaining ambient number densities by use of the Gerdien condenser is a simple matter. Partially ionized gas of known volume flow rate V passes between the condenser plates and an electric field large enough to remove all ions is applied. If e is the electronic charge and n the ion density, the collected current, I, is then related to the number by

$$I = neV . \tag{1}$$

In this mode of operation the collected current is independent of electric field. At lower fields a second mode of operation in which the current is proportional to the applied field yields conductivities instead of number densities. We have not made use of the conductivity mode in the experiments reported here.

Figure 1 is a schematic sketch of the overall Gerdien system. Gas flow is produced by the two blowers which pull air in from the ambient atmosphere. A potential large enough to remove all ions from the air is applied between the collector and voltage plates. Ion current to the collector plate is measured by timing the rate of voltage accumulation on the plate. In flight, a repetitive program of six voltages, three positive and three negative, is applied to the condenser voltage plates.
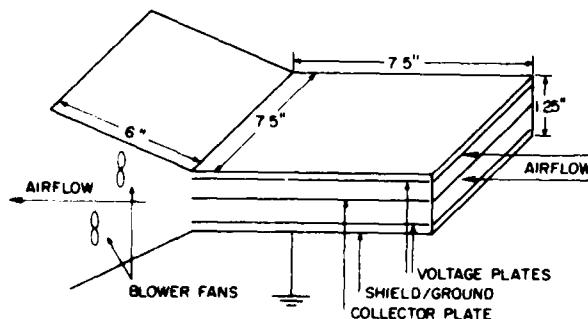
Figure 1. Sketch of Gerdien Condenser System

The final arrangement of electrodes (Figure 2a) evolved from the simpler, more obvious arrangement of Figure 2b with the following improvements:

(1) Effective collecting area is doubled,

(2) Collecting area is shielded from stray capacitances,

(3) P_1 is kept near ground potential, thus simplifying the electrometer (E) design,

8

(4) The shield S partially isolates the ambient from the voltage electrode P_2.

These changes resulted in a compact, well shielded and guarded condenser with simple, reliable sensing circuitry and a convenient voltage switching capability.
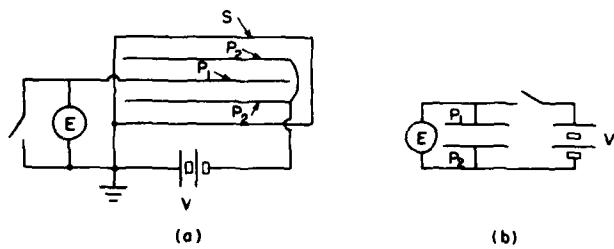
Figure 2. Illustration of Evolution of Electrode
System Leading to Greater Convenience and
Improved Shielding

It was observed on the first flight that currents collected at the highest voltages were frequently lower than those collected at intermediate voltages. This was interpreted as an electric field effect deflecting ions from the voltage electrode directly to the ground surfaces at the inlet. To avoid this, an additional guard electrode was incorporated on the second and sub~~quent flights as shown schematically in Figure 3.
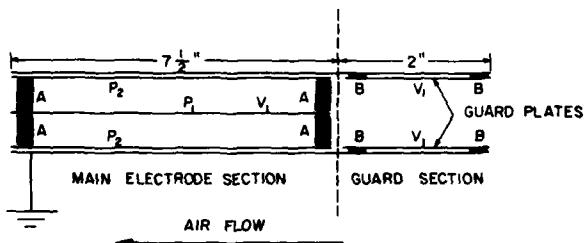
Figure 3. Further Evolution of Collecting/
Shielding Electrode System. Guard plates
are electrically connected to collecting
electrode P_1

Since the extension of the collecting electrode is brought physically close to ground surfaces in the guard, the support insulation at B B B B must be of the same high impedance and dependability as that at A A A A. In addition to the original intended purpose of the guard plates, they also further isolate the voltage plates P_2, from the ambient thus providing what would seem to be rather complete isolation of the voltage plates in this respect.

A photograph of the Gerdien unit, complete with preamplifier stage housing (box on top) and mounting bracket (below) is shown in Figure 4.
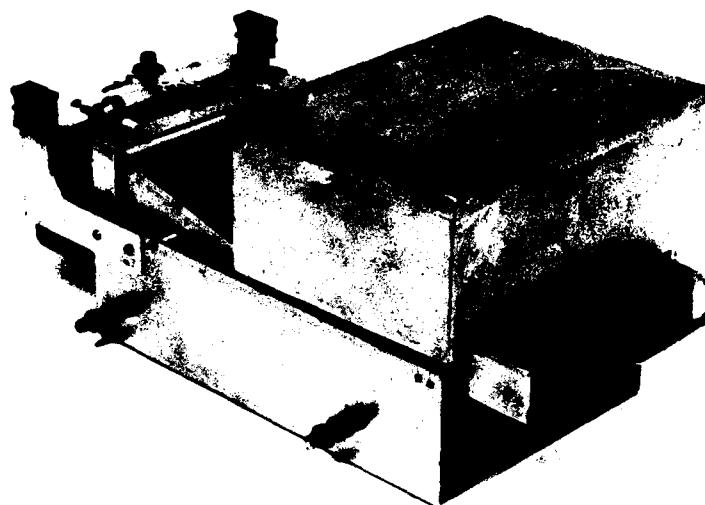
Figure 4. Photo of Gerdien Assembly. Single guard plate showing in front; voltage plates are hidden behind guard section

2.2 Motors and Fans

The blower fans were TRW Globe Motors Vaneaxial type VAX-3-BD. These have a free air flow of 110 cfm (52 ℓ/sec), a peak rated speed of 13,000 rpm, draw, a rated current of 1.5 A at 28 V dc and weight 16 oz each. At altitude the lowered air resistance results in a lower current. Typical flight currents were of the order of 0.25 A for each fan at rated voltages. The advantage to be obtained from higher speeds are substantial, and for the later flights the fans were run at speeds considerably above their rated speed, thus increasing the volume flow rate, especially at higher altitudes.

Calibration of the fans, when completed, will supply volume flow rates as functions of fan speeds and ambient densities. In anticipation of obtaining this information and also as a general fan operation diagnostic, the fan speeds were monitored by use of light emitting/detecting sensors.

To avoid flows induced by ambient wind transients and gradients, a louver system was placed in front of the Gerdien entrance on all but the last flight. Access to the volume immediately in front of the Gerdien entrance is largely free, but direct externally generated winds are blocked off. There is some risk of loss of ions on contact with louver surfaces, but because of the continuum nature of the flow this was not expected to be a serious problem.

Motor/fan units were tested in the laboratory in vacuum at intended flight speeds for periods ranging from minutes up to a full 4 hours. One such test, for 4 hours, was with motor speeds of 20,000 rpm which the unit survived with no apparent ill effects.

2.3 Electronics

Currents are measured by timing the charge rate of the Gerdien condenser. This latter has a capacity of 120 pF. Using a crystal oscillator of nominally 16 kHz the required basic timing increments are obtained by successive doublings of the crystal period. The measuring field consists of 8 bits or 256 basic increments. On later flights the basic increment was changed along with the applied voltages at approximately 30 km. This was intended to accommodate the lowered volume flow rates and attendant lower currents expected at higher altitudes.

The excitation and sensing circuits are illustrated schematically in Figure 5. The programmed bias voltage V_2, is generated by amplifier A_2 and applied to the biased plate(s) of the Gerdien capacitor. The sensor plate is initially shorted to ground by S_1, making $V_1 = 0$, and the charge timer is reset to zero. When the sensor ground is released, the charge timer is enabled and the "interval" for accumulation of charge to 1 V is measured. The GC sensing electrode voltage V_1 is followed by amplifier A_1. The A_1 output is effectively compared with a $\pm$ 1 V reference by comparator C_1 which inhibits timing when $V_1 = 1$ V and the program sequencer is advanced. Also, if the timer reached full scale (255 counts) before 1 V is accumulated, the sequencer is advanced. When the GC is in the autocycle (normal) mode, the mode control advances to the next mode step. (Alternatively a fixed mode may have been selected for indefinite repetition.) A latch L_t retains the timer reading f or telemeter readout until it is reloaded with the subsequent step data.

The autocycle mode is designed to step the program through three positive steps and three negative steps of bias voltage V_2. These voltages are selected by switching preselected resistors into the feedback network of bias amplifier A_2, which

11

multiplies a reference voltage V_0. The voltage V_2 is further made to track V_1 by injecting a tracking reference via resistor R_t, thereby holding $V_2 - V_1$ constant through each mode step.
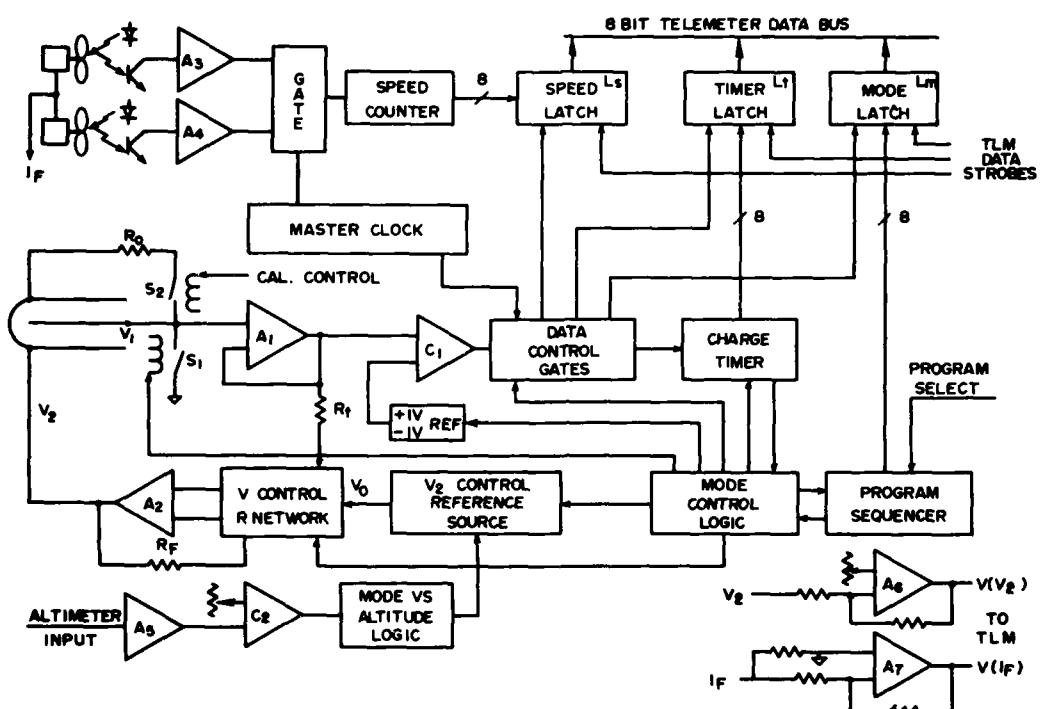
Figure 5. Schematic Block Diagram of Electronics

The three voltages V_2 for each altitude range have been carefully selected to step in a 1:3 relation. This ratio is retained at all altitudes. Further, the high and low altitude steps are selected to overlap, that is, lower low-altitude voltages duplicate higher high-altitude voltages (Section 3.1). The transition between altitude ranges is implemented by scaling the reference voltage V_0, and triggered by comparator C_2 which senses an altimeter input signal through A_5.

Fan (blower) speeds are monitored alternately by optical sensors via amplifiers A_3 and A_4. A clock-controlled gate regulates the speed timer so as to count fan blade transitions during 1-sec gate periods.

12

Most flights included a calibration capability which consisted of an additional, commandable, switch S_2 which inserts a resistor R_o between GC plates. Normal GC operation with fans off (no flow) will produce definite timer counts corresponding to the charging current V_2/R_o. Deviations from this condition provide important clues to anomalous behavior such as may be introduced by leakages, thermal stresses, and so on.

Telemetry data is fed to the telemeter encoder in two ways. Primary timer count data, fan speed count data, and mode/status flags are transferred in 8-bit bytes via a parallel data bus and strobed latches L_t, L_s, and L_m. Additional monitors are presented in analog voltage form. A_6 presents an image of the bias voltage V_2, and A_7 presents an image of the combined fan motor current. The A_6 output contains all principal data under normal operation (at reduced precision), since the voltages V_2 and time lapses may be taken from this display. It consequently functions as a convenient quick-look and backup data channel. The A_7 output provides backup and diagnostic fan performance data.

A typical stripchart display of data from the bias voltage and primary count channels is shown in Figure 6. Indications of bias voltage magnitude and sign, plus typical time intervals are clearly displayed. Dependence of counts on the Gerdien voltage is also seen; this is discussed in more detail in what follows.

3. COLLECTION AND FLOW CONSIDERATIONS

3.1 Collection

In practice, collected currents are found not to be completely independent of electric fields. The most obvious cause of this failure to "saturate" is the effect of fringing fields, and some precautions can be (and have been) taken to try to minimize this effect. Nevertheless, some changes in collected current with applied field persist, and failure to recognize or properly allow for this can lead to erroneous estimates of accuracy. We have attempted to get indications of the magnitude of this effect by stepping the voltages through six increments throughout the flight. (Continuous "ramp" voltages are not practical because of the low current and attendent long response times of the system.)

The voltages used were the following:

Under	~ 30 km altitude	± 2.5 V	± 7.5 V	± 22.5 V
Over	~ 30 km altitude	± 0.8 V	± 2.5 V	± 7.5 V
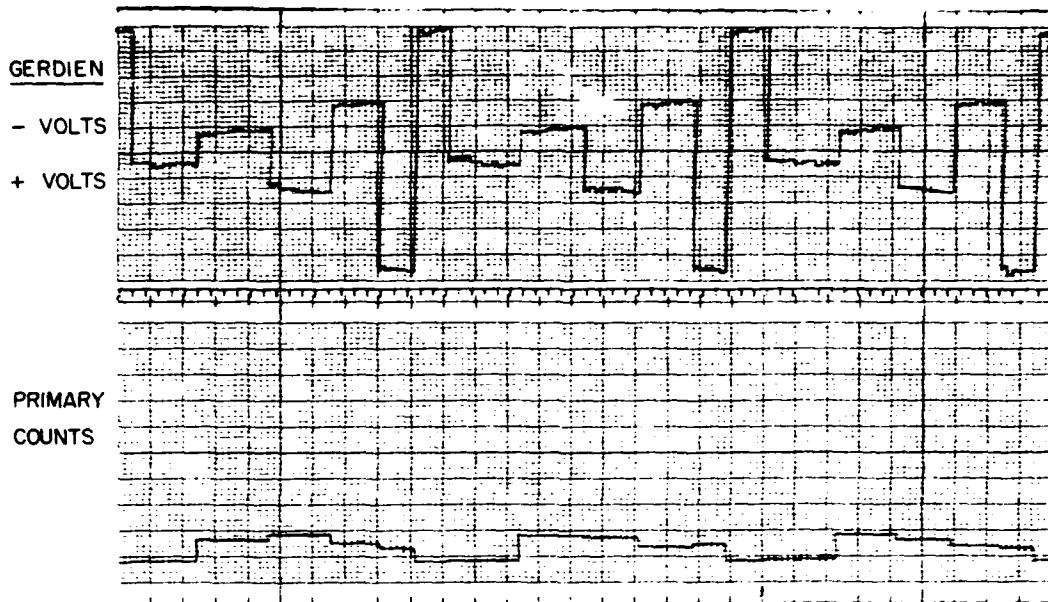
Figure 6. Strip Chart Output for Gerdien Voltages and Primary Counts.
Full counts = 255, single count = 0.1205 sec and chart speed is 2 mm/sec.
Data of 16 May, 1983, at 28 km. Counts correspond to previous voltage
readings

A systematic dimensional analysis of the fluid flow, electric field collection
system is easily accomplished, but many of the dimensionless parameters derived
from this are largely irrelevant (for example, Knudson number, Mach number).
The relevant parameter in the present context is the ratio of characteristic electric
field drift velocity to characteristic fluid flow velocity, V_d/V_o. V_o varies from
~ 1000 cm/sec at 20 km altitude to ~ 300 cm/sec at 40 km. The mobility varies
from ~ 25 cm^2/volt-sec at 20 km (~ 40 Torr) to ~ 500 cm^2/volt-sec at 40 km
(~ 2 Torr). Characteristic maximum electric field strengths (applied voltage/
electrode separation) are 10 V/cm at 20 km and 3 V/cm at 40 km. Thus, the maxi-
mum value of V_d/V_o is ~ 0.25 at 20 km and ~ 5 at 40 km. These numbers confirm
the need for precautions to prevent the applied potential from effecting the collected
current.

3.2 Flow

As noted in the introduction, a major objective of this effort has been to obtain
adequate volume flows through the Gerdien over the altitude range of ~ 20 to 40 km
using readily available commercial devices. Prior to our first balloon flight,

14

laboratory tests of the fan pumping capabilities at reduced densities were performed. For this purpose, the Gerdien/blower system was placed in a bell jar and instrumented with a Pitot tube as shown in Figure 7. A single Pitot tube measurement does not, of course, yield a volume flow rate but only a single velocity of the duct profile. This, however, is only a part of the limitations of the instrument. At low densities the pressures of both static and dynamic ports becomes small; and even more troublesome, the Reynolds number, based on the dynamic tube entrance radius, approaches unity, and there is a breakdown in the Bernoulli law relating velocity and pressure drop. Nevertheless, having said all this, it is still possible to gain a fair amount of information using the Pitot tube.
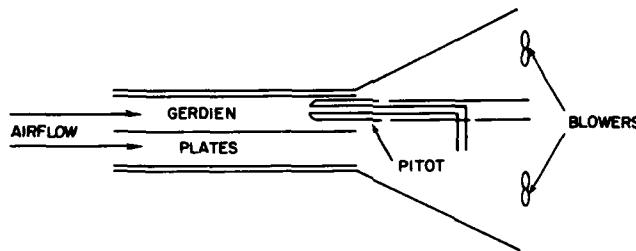
Figure 7. Location of Pitot Tube for Duct Velocity
Measurements

The Bernoulli formula relating velocity to pressure is

$$v = \left(\frac{2 \Delta p}{\rho} \right)^{1/2}$$

(2)

where here Δp is the difference between dynamic and static pressure and ρ the density. Setting

$$\rho / \rho_o = p / p_o$$

where the subscript o refers to some reference condition, we have

$$v = \left(\frac{2 p_o}{\rho_o} \right)^{1/2} \left(\frac{\Delta p}{p} \right)^{1/2} = \left(2 \frac{RT}{M} \right)^{1/2} \left(\frac{\Delta p}{p} \right)^{1/2}$$

where T is the temperature, M the molecular weight and R the universal gas constant.

For $T \cong 300°$ and $R/M = \dfrac{8300}{29} = 286$ (m/sec)^2/deg

$$v = 414 \left(\frac{\Delta p}{p}\right)^{1/2} \text{m/sec} . \tag{3}$$

Now the free air flow of the fan is ~ 5 m/sec. The minimum pressure differential which it will be required to measure is thus of the order

$$\Delta p) \cong 10^{-4} \, p_{min} = 2 \times 10^{-4} \text{ Torr} .$$

Pressure differences of this order can be measured with an MKS Baratron gauge, model 170M25B.

As far as the breakdown of Bernoulli's law is concerned, the situation is as follows.[2] The law may be used without correction down to a Reynolds number of ~ 3. Below Re = 3 one can obtain only rough estimates by extrapolating the correction curve. Two Pitot tubes of different sizes were used, the larger to increase the Reynolds number at the lower densities. The results of these measurements are shown in Table 1. * are extrapolated values and a is the Pitot inlet orifice radius. The quantity here designated by Δp is labelled P - p in Figure 8.

Table 1. *Duct Velocity-Ambient Pressure Relations Obtained in Laboratory Tests*

Pressure (Torr)	Equivalent Altitude (km)	Δp (Torr)	a (cm)	v/v_o	Re	c_p
2	40.8	0.00023	0.0794	0.386*	0.205*	6.3*
4	35.6	0.00033	0.0794	0.455*	0.48*	3.25*
8	30.7	0.00075	0.0794	0.654*	1.4 *	1.77*
16	26.0	0.0018	0.0597	0.836	3.55	1.3
32	21.6	0.00425	0.0597	0.957	8.13	1.13
64	17.2	0.00835	0.0597	1.0	17	1.06

2. Bryer, D.W., and Pankhurst, R.C. (1971) Pressure-probe Methods for Determining Wind Speed and Flow Directions, Her Majesties Stationery Office, London.

$C_p = (P-p)/\frac{1}{2}\rho V^2$
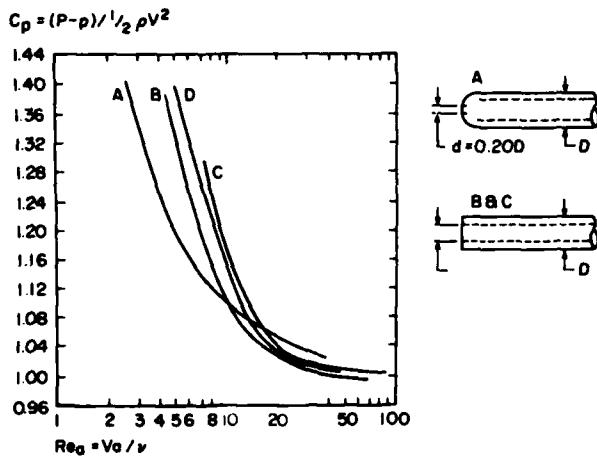
Figure 8. Pressure Coefficient (correction factor) C_p vs Reynolds Number Re as Taken From Bryer and Pankhurst (A is applicable curve)

The values in the last three columns are obtained as follows. Figure 8, reproduced from Reference 2, gives corrections to the Bernoulli law (c_p = pressure coefficient) as functions of Reynolds number. This Reynolds number, however, is based on **true** velocity, and hence

$$c_p (Re) = \frac{\Delta p}{1/2 \, \rho v^2} \tag{4}$$

is an implicit equation for v. We choose a simple approximation to c_p as a function of Re,

$$c_p = 1 + \alpha/Re$$

and by matching at Re = 3, find

$$c_p = 1 + \frac{1.08}{Re} \ .$$

The equation for determining v is, then, making use of the ideal gas law and ignoring variations in temperature

$$(v/v_o)^2 + \frac{\alpha}{Re)_o} \left(\frac{p_o}{p} \right) \frac{v}{v_o} - 2/v_o^2 \ \frac{\Delta p}{p} \frac{RT}{M} = 0 \ . \tag{5}$$

17

Here, the subscript zero refers to reference values chosen as the values at $p_o = 64$ Torr (velocities not differing appreciably from those at sea level) and $v_o = 4.6$ m/sec,

$$Re)_o = 17, \quad RT/M = 8.58 \times 10^4 \ (m/sec)^2 \ .$$

Solving the quadratic equation we have

$$2 \frac{v}{v_o} = -0.0635 \left(\frac{p_o}{p} \right) + \left[0.00404 \left(\frac{p_o}{p} \right)^2 + 3.20 \times 10^4 \ \frac{\Delta p}{p} \right]^{1/2} \ .$$

(6)

From v/v_o, we obtain

$$Re = Re)_o \ \left(\frac{p}{p_o} \right) \left(\frac{v}{v_o} \right)$$

and thence $c_p = 1 + 1.08/Re$.

As far as required volume flow rates are concerned, there seems to be no question up to altitudes of ~ 30 km. Here, the corrections are known, and the decrease in volume flow rate is only about 35 percent. Above 30 km, the correction factor is based on extrapolation and the results are uncertain. Still, it would be surprising if the predicted flow ratios were not correct to within a factor of 2 or 3. If the volume flow rates at 40 km were as predicted, ~ 1/3 of those at sea level, this would provide an adequate supply of ions. The prognosis for obtaining adequate flow rates with the blower fans is thus favorable.

Expectations of increased flow with increases in fan speed can be inferred on dimensional grounds. Even at peak altitudes (~ 40 km) the ratio of mean free path to fan blade characteristic dimension is small (~ 10^{-3}) and so the volume flow rate depends only on the Reynolds number. The volume flow rate can then be expressed as

$$V = A_f v_f \ F \ (Re) = A_f v_f \ F \ \left(\frac{\rho v \ L_f}{\mu} \right)$$

(7)

where

A_f = fan throat area
v_f = velocity of fan blade tip
ρ = density of air
L_f = fan blade characteristic dimension
μ = coefficient of viscosity

and F is an arbitrary function.

18

If we let subscripts refer to altitudes (or densities) and superscripts to fan blade speeds, we have

$$V_1^1 = A_f v_f^1 \, F\left(\frac{\rho_1 v_f^1 L_f}{\mu}\right) \tag{8a}$$

$$V_2^1 = A_f v_f^1 \, F\left(\frac{\rho_2 v_f^1 L_f}{\mu}\right) \tag{8b}$$

$$V_1^2 = A_f v_f^2 \, F\left(\frac{\rho_1 v_f^2 L_f}{\mu}\right) \tag{8c}$$

$$V_2^2 = A_f v_f^2 \, F\left(\frac{\rho_2 v_f^2 L_f}{\mu}\right). \tag{8d}$$

If we set $\rho_1 v_f^1 = \rho_2 v_f^2$, we obtain the scaling law

$$V_2^2 = V_1^1 \, v_f^2 / v_f^1 . \tag{9}$$

If for example, $v_f^2 \cong \alpha \, v_f^1$ (and $\rho_2 = 1/\alpha \, \rho_1$), we obtain a flow rate α times the old rate, not at the old altitude, but at the higher (if $\alpha > 1$), new altitude. The gain in flow obtained by increasing the fan speed is thus expected, especially at higher altitudes, to be substantial.

3.3 Ambient Velocities

With regard to the influence of ambient velocities the situation is much more complicated. Even without the fan, flow through a duct depends on both Reynolds number (based on ambient velocity) and duct dimensions. With the fan, an additional Reynolds number, characterizing the behavior of the fan, must be added to specify the overall flow. The two velocities, that is, the ambient as well as the mean duct velocity induced by the fan, are certainly not simply additive in obtaining overall duct velocities. In fact, it is not even clear that duct velocities without the fan, and velocities induced by the fan, are additive. Solution of this problem requires further study and will probably remain, to some extent, dependent on observational data. The relative influence of ambient velocities will clearly be reduced by increasing the fan speed.

19

4. FLIGHT DATA

4.1 General Comments

Table 2, a listing of the five flights on which the Gerdien was included, gives some of the features and changes within the instrument on these flights. Data was obtained on all but one of these flights. Because the purpose of these flights was largely to check out the potentialities of the instrument, we do not present all the data obtained but confine ourselves largely to the 16 May 1983 flight. On that flight the fans were run at high speed, there were no fan failures, and data was obtained at altitudes up to approximately 38 km.

Table 2. Summary of Flight Features

Flight Date	29 Sept 81	21 May 82	4 Oct 82	16 May 83	24 June 83
Approx. fan speed (rpm)	12,000	12,000	20,000	20,000	20,000
5×10^{11} Ω calibration resistor	No	Yes	Yes	Yes	Yes
Front end louvre	Yes	Yes	Yes	Yes	No
Front end guard	No	Yes	Yes	Yes	Yes
Basic timing increment (sec)	0.964	0.1205	0.1205	0.1205 <30 km 0.482 >30 km	0.1205 <30 km 0.482 >30 km
Comments	System T.M. failed at 24 km on ascent.	Instrument sensitivity lim. data to under 30 km.	No data-cal resistor shorted across electrometer input - one fan motor failed (brush disintegrated).	Generally good data - fan motor indicator showed possible trouble with one.	One fan motor failed (brush disintegrated).

4.2 Leakage and Calibrations

The term "apparent leakage" is used here to refer to currents obtained with the motor off and the calibrating relay open. Rosen[1] attributes a similar "motor off" current to turbulence bringing new ions into the collector. In the present experiment there are good reasons to believe that this is a leakage rather than an ion current. Table 3 shows the data pertinent to the leakage problem. In the calibrate

20

mode, a fixed resistor, nominally of 5×10^{11} Ω, is switched by a reed relay into the input of the electrometer. It thus appears effectively in parallel with the plates of the capacitor. In the apparent leakage mode, the motors remain off and the relay is opened. Figure 9 shows the equivalent circuit for analysis. There are two sources of leakage currents considered, a leakage across the relay, R_1, and a leakage in parallel with the capacitor plates, R_2.
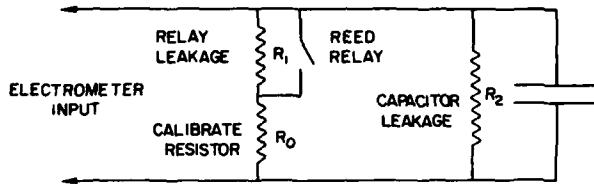

Figure 9. Equivalent Circuit for Leakage Analysis

In ground tests the apparent leakage is largely absent. It appears in flight, on instrument turn on, and as seen in the table, tends to disappear again after long residence times at higher altitudes. For higher altitudes, noting that counts are proportional to resistances, we observe that

$$R_2 > \frac{(R_o + R_1) R_2}{(R_o + R_1) + R_2} >> R_o \tag{10}$$

and hence that $R_2 >> R_o$. We also note that R_o as measured in the CAL mode, is close to the nominal value of 5×10^{11} Ω. At lower altitudes, where leakage plays a role, we have

$$\frac{R_o R_2}{R_o + R_2} = R_{CAL} = R_C \tag{11}$$

$$\frac{(R_o + R_1)R_2}{(R_o + R_1) + R_2} = R_{LEAKAGE} = R_L . \tag{12}$$

From measured values of R_C and R_L we then obtain R_1 and R_2, the equivalent leakage resistances. We have, solving Eqs. (11) and (12)

$$R_2 = \frac{R_c R_o}{R_o - R_C} \tag{13}$$

$$R_1 = \frac{R_o^2 (R_L - R_C)}{R_C R_o - R_L R_o + R_L R_C} \quad . \tag{14}$$

For a typical case using counts, we have for the flight of 24 June 1983 at 7.5 V,

$$R_o = 20, \quad R_L \cong 86/4 = 21.5, \quad R_C \cong 74/4 = 18.5 .$$

Then $R_2 = 247$ counts.
Since $R_o = (20 \text{ counts}) = 5 \times 10^{11} \, \Omega$,

$$R_2 = \frac{247}{20} \cdot 5 \times 10^{11} = 6.2 \times 10^{12} \, \Omega.$$

Similarly, $R_1 = 3.5$ counts

$$= \frac{3.5}{20} \cdot 5 \times 10^{11} = 8.7 \times 10^{10} \, \Omega.$$

It is thus clear that of the two contributions to the apparent leakage, the leakage across the relay plays the dominant role. Similar computations for the 16 May 1983 flight lead to the same conclusion.

The argument for identifying these currents with leakage rather than ion currents is the following. In the mobility mode, the ion currents for plus and minus voltages of equal magnitude are not, in general, equal. The ± currents in Table 3, on the other hand, are close to equal. In the number density mode ion currents are not proportional to voltages. The currents in the table are roughly proportional to voltages. Thus, the observed currents are incompatible with either mode of ion collection; they are compatible with leakage currents.

In a recent flight (6 Oct 1983) for which data has not yet been reduced, the reed relay was removed from the circuit before launch; there was thus no calibrate mode. With the motor off, all counts went off scale, a further indication that the "apparent leakage" was, in fact, leakage across the reed relay. For the present flight data, the leakage currents are subtracted from measured currents to obtain true ion currents.

Table 3. Counts Obtained in "Calibrate" and "Leakage" Modes

16 May 1983, Holloman AFB, Gerdien Data

Voltage	Calibration								Apparent Leakage							
Alt:	+0.83	-0.83	+2.5	-2.5	+7.5	-7.5	+22.5	-22.5	+0.83	-0.83	+2.5	-2.5	+7.5	-7.5	+22.5	-22.5
18.3			204	204	68	68	24	24								
19.0											255	255	103	96	35	36
20.4			208	208	68	68	24	24								
21.5											255	255	94	94	33	34
24.2			209	212	70	71	24	24								
24.7											255	255	104	101	34	35
27.0			219	213	70	71	24	25								
27.2											255	255	103	101	34	35
32.3	239	171	55	53	18	18										
33.0	192	171	53	53	18	18										
33.7									255	255	87	79	27	26		
37.8	255	169	57	53	18	17										
37.9	226	166	55	53												
37.9												255	132	82		
38.3	255	207	55	50	16	16										

23

4.3 Blower Fans

The requirements on the motor/fan units are that they produce an adequate flow at all altitudes of interest; that this flow be relatively independent of ambient wind velocities, and that the units perform dependably throughout the duration of a flight. Of these three requirements, that of producing an adequate flow at all altitudes seems to have been satisfied. Predictions that the volume flow would not decrease by more than a factor of approximately three at peak altitudes of roughly 40 km have been confirmed.

As far as dependability goes, there were no motor failures for the fans operated at rated speeds of 13,000 rpm. Of the motors run at 20,000 rpm, with three flights and two units per flight, there were two motor failures. The two failed motors showed excessive brush wear and graphite powder was dispersed throughout the unit. This seems to be a go, no-go, phenomena; the motors which did not fail showed no visible brush wear and remained completely free of graphite powder. The unit tested in the laboratory for four hours at high speeds showed no brush wear.

It has recently come to our attention that there are brushes specially fabricated for high altitude applications. Since our operation with standard brushes resulted in the majority of brushes surviving, it seems likely that use of the special brushes will eliminate the problem of sudden excessive brush wear.

The question of dependence of flow on ambient velocities is still open. As will be shown in the following section, sensible fluctuations in ion current do occur; whether these are due to unsteady flow rates, to genuine changes in number densities, or to a combination of the two, cannot be decided without further study.

4.4 Ion Collection Data

Data reduced from the flight of 16 May 1983 is shown in Figures 10, 11, 12, and 13. In all these figures the data has been corrected for leakage which generally amounted to roughly half of the original counts. Data is presented for an assumed flow velocity of 10 m/sec (60 ℓ/sec flow), and so, only relative values of number densities are of significance. The absolute values are, however, in the range reported for other measurements.[1] Figures 10 and 11 are for an assumed constant flow rate, while Figures 12 and 13 are for a flow corrected for altitude (or density) as explained in Section 3.2. Also drawn on all four figures are linear least square fits for various Gerdien voltages. There are three aspects of this data which we will discuss: (1) scatter and its possible relation to ambient flows; (2) altitude/volume flow rate effects; and (3) electric field effects.

24
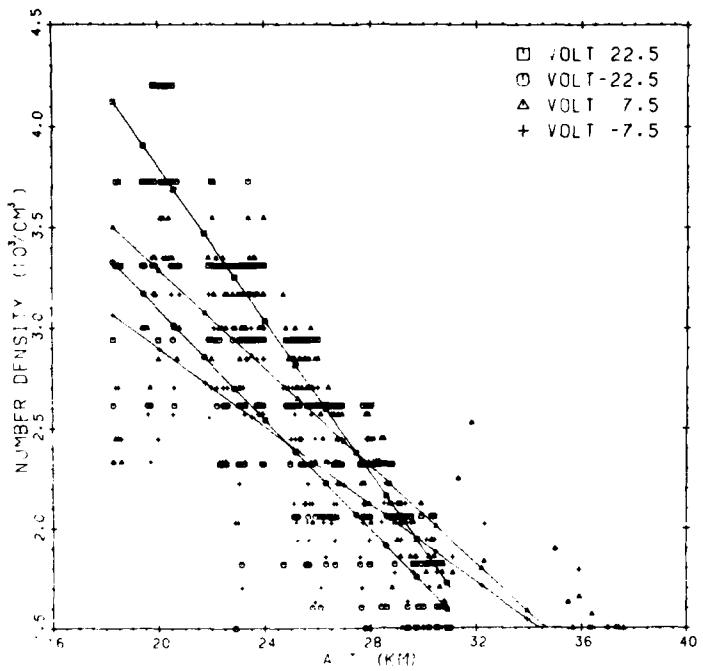
Figure 10. Ion "Number Densities" vs Altitude for
an Assumed Flow Velocity of 10 m/sec in the Density
Mode

Of these three, the second, although of interest in its own right is least
important, since ultimately a flow calibration will answer most questions dealing
with altitude effects on the volume flow rate. The numerous segments of Figure 10
showing sustained constant densities over many readings are due at least in part
to (digitized) readings occurring in the lower part of the count range. The curvature
evident in Figure 12 is generated by the flow altitude correction. We note that some
clusters of adjacent reading show a rise of between 0.2 and 0.3 on the ordinate
scale. If the volume flow did actually decrease enough to justify a correction, it
would be sufficient to produce changes in the counts, since densities are known to
also decrease with increasing altitude at these altitudes. This, as seen in Figure 10,
we do not observe. The possibility is thus suggested that we are over-correcting
for the altitude change in flow rate. If true, the performance of the fans at high
altitudes would be even better than predicted. In any event, these questions will,
as noted, be answered by a proper calibration.

We next turn to the question of scatter. Root mean square deviations from the
linear fits are all of the order of $0.3 \times 10^3/cm^3$. Thus, for the number density data
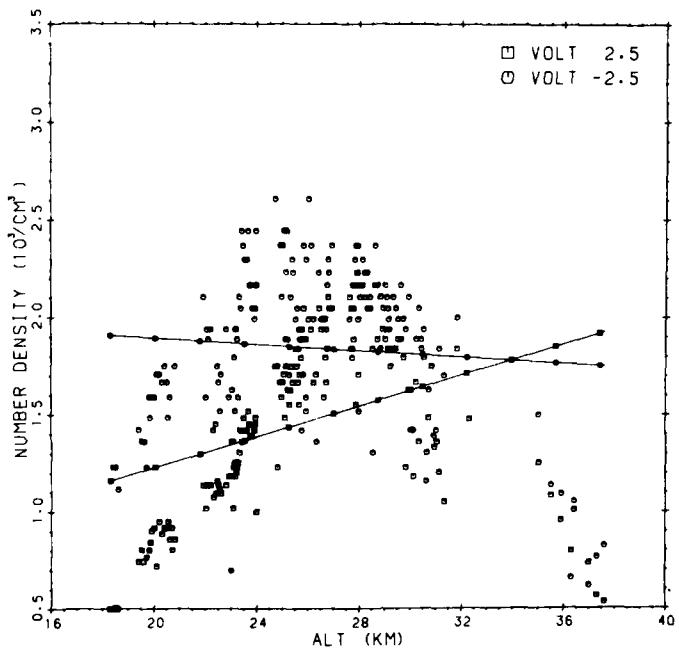
Figure 11. Ion "Number Densities" vs Altitude for an
Assumed Flow Velocity of 10 m/sec in the Mobility
Mode

corrected for flow (Figure 12) the rms deviations are roughly 10 percent of measured
values and represent a fair accuracy. For the uncorrected data (Figure 10) the
rms deviations are at worst (upper altitudes) approximately 20 percent of measured
values. Since need for some correction is very likely, the rms deviations are
expected to be rather closer to 10 percent than to 20 percent of average values. If
this scatter is caused by variations in flow rate induced by ambient winds, it can
arise in more than one way. First, we may imagine the mean ambient wind to have
no velocity gradient, in which case the platform experiences no mean velocity. In
this case, a variable component of ambient wind may be generated by turbulence.
Second, there may be a gradient in the mean ambient wind, and this, combined with
a rotation of the instrument platform will also generate apparent variable ambient
winds. The rotation of the platform is somewhat erratic, but generally the time of
a single revolution is of the order of one minute. Since the platform can perform
many revolutions between reversals, the period of oscillation could thus easily be
many times longer than this. Typical measurement times are on the order of 0. 2
to 2 min and so this type of motion could account for the appearance of the data;

26
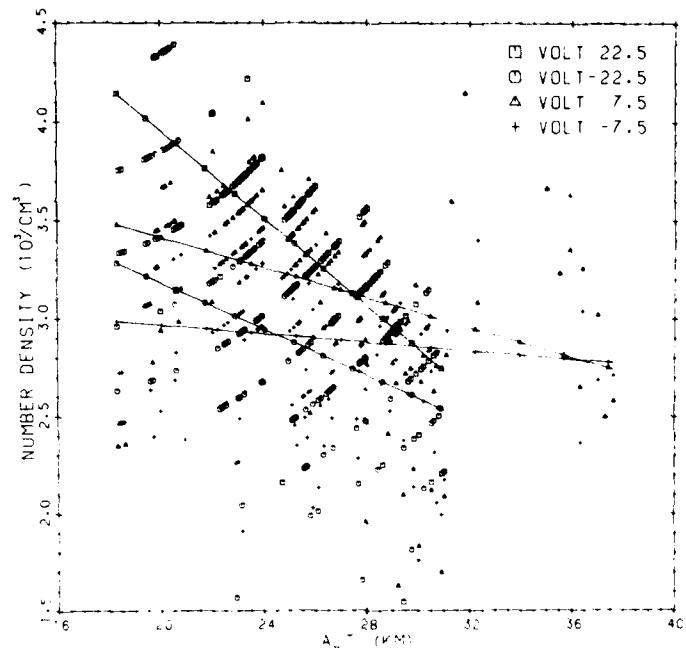
Figure 12. Ion "Number Densities" vs Altitude for an
Assumed Flow Velocity of 10 m/sec in the Density
Mode; Corrected for Altitude Flow Dependence

closely spaced clusters in the absence of ambient gradients or at the stationary
points of oscillation, and more widely scattered readings otherwise. It is expected
that turbulence plays a lesser if any role in generating scatter.

The flight of 24 June 1983 was the one flight in which the front end louver was
not present. Data from this flight has not yet been reduced but a cursory inspection
leads one to conclude that there are no major differences between the data from this
and other flights as far as scatter is concerned. Thus, either the louver is not very
effective in suppressing ambient wind effects or the scatter is not due to ambient
winds. In either case the louver will probably not be included in future flights; it
must show a marked improvement in performance to justify its inclusion in the face
of other possibly detrimental effects.

Turning now to electric field effects we note the radical differences between
Figures 10 and 12 on the one hand and Figures 11 and 13 on the other. A compari-
son of Figures 12 and 13 shows that the latter represents a mobility mode. The
collected current increases with increasing altitude, is generally lower than the
current at corresponding altitudes for the higher voltages, and is higher for the
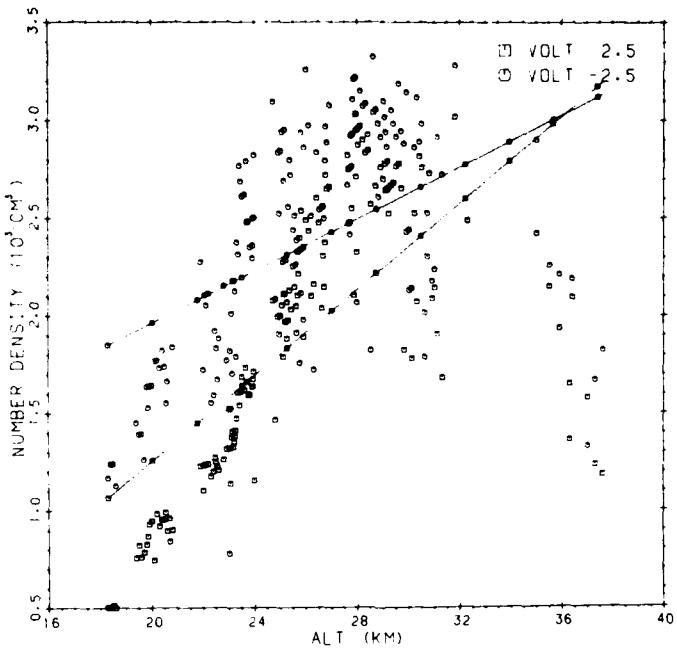
Figure 13. Ion "Number Densities" vs Altitude for an
Assumed Flow Velocity of 10 m/sec in the Mobility
Mode; Corrected for Altitude Flow Dependence

negative than for the positive voltages (compatible with a higher positive ion mobility).
At the higher altitudes the currents become comparable to those collected with the
higher voltages, an indication of the onset of saturation. The higher voltages (Fig-
ure 12) shows a general decrease in current with altitude, and this is in accord
with previously published number density measurements.[1] The differences in
current with voltages are, however, of the order of the rms deviations, conse-
quently real, and so require consideration. We note first that the readings at
+22.5 V are larger than those at -22.5 V and likewise for the readings at +7.5 V
and -7.5 V. This is opposite to what is found at 2.5 V and makes mobility considera-
tions unlikely as a cause of the differences. Furthermore, the currents for +7.5 V
are larger than those for -22.5 V; this precludes an explanation in terms of a vehicle
charge shifting the zero of potential. As discussed earlier, some care has been
taken to avoid the fringing field of collecting electrodes, and yet these electric field
effects persist. At present we do not have an explanation for their cause. Averaging
the number densities for all four voltages would give a single mean number vs
altitude profile with a maximum error of about 0.5 in 3.5×10^3 or roughly 15 percent.

5. CONCLUSIONS

Other methods of obtaining volume flows through Gerdien condensers such as with the lobe type pump have their own inherent limitations. The use of the blower fans appears, in the light of the present work, as a viable alternative having both advantages and disadvantages. On the credit side is the ready availability of the fans as well as their higher flow rates which result in a system having an inherently higher signal. The ratio of volume flow to required power also seems to be higher for the blowers than for the lobe pumps. For example, one report of the latter[1] indicates a 2ℓ/sec flow and a power requirement of 3W while our fans have flow rates of 50ℓ - 100ℓ/sec and use ~ 12W. On the debit side is the necessity for independent calibration of the fans and also the as yet unanswered question of the steadiness of flow in the presence of ambient velocities. The former can be treated by a straightforward, though not necessarily negligible, effort; the latter requires further investigation.

END

FILMED

8-84

DTIC